Effects of dehydration on the apolar surface energetics of inorganic paper fillers[☆]

William M. Burry, D. Steven Keller[*]

Empire State Paper Research Institute, Faculty of Paper Science and Engineering, State University of New York College of Environmental Science and Forestry, 1 Forestry Drive, Syracuse, NY 13210, USA

Abstract

The surface energies of various inorganic fillers including kaolin clay, titanium dioxide, and talc were examined using inverse gas chromatography (IGC). In an earlier investigation that examined calcium carbonate fillers, dehydration by heating under a dry nitrogen purge had a substantial influence on the apolar (γ_S^{LW}) and polar (γ_S^{AB}) components of surface energy as measured using IGC. Using the same approach, the influence of such conditioning on several inorganic fillers used in papermaking were determined using preconditioning IGC from 100 to 300 °C, and sequential isothermal analysis at 100 °C. Results from IGC analysis of titanium dioxides (rutile and anatase) were similar to precipitated calcium carbonate (PCC) for temperatures up to 200 °C. PCC was significantly more energetic after preconditioning at 300 °C, which may indicate the onset of significant thermal decomposition that titanium dioxides will not exhibit. Kaolin clay samples had relatively high apolar surface energy similar to that of the chalk samples. Calcination gave lower γ_S^{LW} values that could not be accounted for by changes in the microporous structure. More likely the differences resulted from contamination of highly energetic surface sites with adsorbates other than water. Talc samples exhibited relatively high apolar surface energies that increased with preconditioning temperature. The results provided insight into the significance of water on the final adhesion properties of fillers in the sheet structure or coating layer.
© 2002 Elsevier Science B.V. All rights reserved.

Keywords: Inverse gas chromatography; Surface free energy; Thermodynamic parameters; Paper; Calcium carbonate; Kaolin clay; Titanium dioxide; Talc

1. Introduction

The surface chemistry of composite materials is of principal importance for the adhesion properties that affect internal bonding, web strength, and wetting properties of liquids such as coatings, adhesives and water. While the application of surface coatings can improve sheet strength and uniformity, the chemistry of the underlying basestock affects the process and the final properties of such applications.

The utility of inverse gas chromatography, IGC, in providing insight into the surface energetics has been demonstrated for a variety of the components that comprise composite materials such as paper. These have included cellulosic fibers [1,2], wood fibers [3,4], and calcium carbonate [5–7]. Numerous other

investigators have used IGC and other methods to study the surface energetics of papermaking materials [8–15].

Our investigation of mineral pigments began with precipitated calcium carbonate, PCC, and its interaction with alkyl ketene dimer, AKD, in response to the rapid growth of alkaline papermaking [5]. The work sought to improve understanding of the surface chemistry of PCC and how that influences problems such as increased sizing demand and sizing reversion. In a study that used IGC to compare natural and synthetic calcium carbonate fillers, substantial differences in the apolar [6] and polar [16] components of surface energy were observed. More importantly it was discovered that thermal conditioning and the amount of surface water had a significant influence on the apparent surface energetics of the fillers from ambient to a state of dehydration. As a result of that investigation, a model was proposed to explain the increased affinity of non-polar alkane probes for the surfaces as water desorbs from the surface during thermal conditioning. A review of the work by Keller and Luner conducted on $CaCO_3$ that considered induced dipole interactions was previously reported [7].

Calculation of the thermodynamics of adsorption from IGC analysis is based on the determination of the specific retention volume, V^0, of a known adsorbate probe as it passes through a chromatographic column containing the adsorbent of interest. The specific retention volume is essentially the volume of carrier gas needed to thoroughly elute the adsorbate, less the dead volume of the column, per unit mass or surface area of adsorbent. For the analysis of solid surfaces, as in the present study, specific retention volume is expressed in terms of specific surface area, V_S^0.

The area specific retention volumes and mass are related to the retention time, t, of injected probes and the specific surface area, A_{sp}, by the relationship [13]:

$$V_S^0 = \frac{V_S^0}{A_{sp}} = \frac{jF_{col}(t_p - t_m)}{A_{sp}w} \tag{1}$$

The subscripts p and m identify the retention times of the probe and a non-interacting marker, respectively. The parameter w is the mass of adsorbent in

the column, j represents the James–Martin correction for compressibility, and F_{col}, is the flow-rate of carrier gas within the column that has been corrected for column temperature. A more detailed discussion of experimental parameters is given elsewhere [5,8].

For analysis at infinite dilution (or zero coverage), specific retention volume may take the form:

$$V_S^0 = \frac{K_S}{RT_C} \tag{2}$$

where R is the gas constant, T_C is the column temperature and K_S is the Henry's Law constant (partition coefficient).

The standard molar free energy of adsorption, ΔG_A^0, of the probe on the adsorbent is related to specific retention volume by the relationship:

$$\Delta G_A^0 = -RT \ln V_S^0 + C \tag{3}$$

The integration constant, C, is a function of these parameters and may be assumed constant for a given adsorbent and a homologous series of probes.

When non-polar molecules, such as n-alkanes are used as probe gases in IGC, the energetics of adsorption are considered non-coulombic and result entirely from Lifshitz–Van der Waals (LW) interactions. The LW contributions to the surface free energy, γ_S^{LW}, encompasses the electromagnetic interactions including the dispersive (London), γ_S^d, induction (Debye), γ_S^i, and orientation (Keesom), γ_S^μ, components so that:

$$\gamma_S^{LW} = \gamma_S^d + \gamma_S^i + \gamma_S^\mu \tag{4}$$

In the case of IGC experiments conducted at exceedingly low concentrations of of the gaseous probe (infinite dilution), the pairwise-addition approximation [17] provides a means to interpret the significance of each separate component to the overall LW interaction. The assumption in this case is that intermolecular distances between probe molecules are large and the Debye and Keesom components are not suppressed by neighboring molecules as in condensed phase-condensed phase interactions, e.g., liquid–solid or solid–solid. This concept has a substantial impact on the widely applied approach of Dorris and Gray [13] for estimating the London-

dispersive component of surface free energy, γ_S^d, from IGC data.

The method proposed by Dorris and Gray involved the use of Fowkes [18] equation for the work of adhesion of a non-polar liquid and a surface, in terms of the incremental change in free energy per methylene group, $\Delta G_A^{CH_2}$. Values for $\Delta G_A^{CH_2}$ are accessed from the difference in for adjacent members of a homologous series of linear alkanes from the relationship:

$$\Delta G_A^{CH_2} = -RT \ln\left(\frac{K_S^{n+1}}{K_S^n}\right)$$
$$= -RT \ln\left(\frac{V_S^{n+1}}{V_S^n}\right) \qquad (5)$$

$\Delta G_A^{CH_2}$ values are determined graphically as the slope of a plot of V_S^0 vs. the number of carbons in the alkane, n. The equation that was derived may be rearranged to solve for γ_S^d so that:

$$\gamma_S^d = \frac{1}{\gamma_{CH_2}} \cdot \left(\frac{\Delta G_A^{CH_2}}{2Na}\right)^2 \qquad (6)$$

where N is Avogadro's number, a is the cross sectional area of the methylene group (6 $\overset{\circ}{A}{}^2$) and γ_{CH_2} is the surface energy of a solid consisting of only –CH$_2$– groups, i.e., polyethylene.

Since the interactions of the alkanes with the surface will involve all of Lifshitz–Van der Waals interactions, the solution to Eq. (6) is more appropriately given as γ_S^{LW} [19]. Furthermore, since the probes are in the dilute gaseous state, the Debye induction interactions, γ_S^i, that result from dipoles induced in the alkane molecules by the electric fields at the adsorbent surface, may be considerable [17], especially for high energy materials such as mineral fillers [20]. It is evident that Dorris and Gray considered the significance of the induction forces even for the low energy cellulosic surfaces that they studied [13]. The assumption that the interaction of gaseous alkanes with low energy surfaces, absent of appreciable electric fields, are dominated by dispersive (London) interactions may indeed be valid. It should be noted that for the alkane/solid system, the Keesom orientation term, γ_S^μ, is zero since *n*-alkane probe gases do not possess a permanent dipole. Therefore, results from the sorption of dilute gas

probes with highly energetic surfaces will likely show appreciable Debye induced-dipole interactions that cannot be neglected, even for non-polar alkane probes.

The present work extends the earlier investigation of Keller and Luner [6,7] that examined CaCO$_3$ to characterize the surfaces of other filler/pigments, such as kaolin clay and titanium dioxide, which are important in the production of composites. Other investigators have used IGC analysis to study a wide variety of minerals including clay [21,22], silica [23], calcium carbonate [24,25], slate [26], mica [27] and talc [28]. While investigators have used IGC at infinite dilution to examine the acid–base nature of surfaces or at finite concentration to attain adsorption isotherms, few have studied the effect of surface water concentration on the observed surface energies [29,30]. Adsorption isotherms and heats of immersion have been used to study the effect of chemisorbed and physisorbed water concentrations on the surfaces of titanium silica [31], zinc oxide [20,32], and calcium carbonate [33]. Suda and Morimoto calculated the effective electrostatic field strength, and the influence it would have on interactions with polar and non-polar molecules [20,34].

Of primary interest in paper material science is the characterization of the composite constituent interfaces in a substantially hydrated state, whether fully saturated, as in experiments examining wet end processes, or at moderate ambient moisture conditions where the properties of use are most relevant. Therefore, developing an understanding of the tenacity of the surface water, and its affect on interactions at the surface has significant practical value for predicting and optimizing adhesion and wetting behavior.

The object of this investigation was to determine the apolar surface energetics of typical inorganic fillers and pigments using inverse gas chromatography at infinite dilution. Consideration of the response of the surfaces to thermal preconditioning would also be examined. The specific objectives were to use IGC to analyze titanium dioxide, kaolin clay and talc samples of various origins. The apolar component of surface free energy, γ_S^{LW}, was measured at different preconditioning temperatures to determine if characteristic trends based on chemical structure or pre-treatment existed. Sequential iso-

thermal analysis of different samples was used to assess the kinetics of changes in surface energetics as steady state was attained. The significance of properties such as crystal structure or thermal structuring (calcination) was also examined in this study.

2. Experimental

2.1. Materials

The filler samples that were studied are identified in Table 1. The calcium carbonate samples, PCC (Albacar 5970, Specialty Minerals, Bethlehem, PA, USA) and chalk (Omya, Alpharetta, GA, USA), were the subjects of earlier investigations [6] the results of which are included for comparison. Three titanium dioxide samples (Millenium Inorganic Chemicals, Olympia Fields, IL, USA) were tested. The first two were commercial filler/pigments representative of the two crystal forms: Rutile (RCL-4) and Anatase (RG). The Rutile sample was manufactured by the chlorine process [35] and had an alumina surface treatment. The Anatase sample was created by the sulfate process [35] and had no additional surface treatment. The third sample, identified as Rutile-Raw, was collected from the kiln discharge of the

Rutile manufacturing process prior to any surface treatment that may affect the surface properties. Four kaolin clay samples were selected in order to study the effects of crystallinity and calcination treatment. Two samples of Georgia kaolin were obtained from the Clay Minerals Society Source Clay Repository (CMS-SCR), Columbia, MO, USA. The first sample, Kaolin-Cr, was well crystallized kaolin and was identified by the CMS-SCR as KGa-1b [36]. The second sample, identified in this report as Kaolin-Am, was poorly crystallized (amorphous) and was identified by the CMS-SCR as KGa-2.

The well-crystallized kaolin sample, Kaolin-Cr, was heat treated (calcined) in the laboratory at 900 °C for 4 h. The product of this treatment is identified as Kaolin-Cr/Cal. The last kaolin sample, identified as Kaolin-Cal, was obtained commercially as a calcined product (Hycal, J.M. Huber, Atlanta, GA, USA). Talc samples were obtained from Specialty Minerals as a milled product, Talc-Prod, and in nugget form. The talc nuggets were steatite ore from Montana. The sample identified as Talc-Raw was ground by hand in the laboratory without milling aids or additives. In order to prepare samples for inverse gas chromatographic columns, all samples had to be aggregated under pressure and screened to isolate the 400×250 μm size fraction. Using this

Table 1
Inorganic paper fillers

Sample	Specific surface area ($m^2 \cdot g^{-1}$)	Cumulative pore volume ($\cdot 10^{-3}$ cm^3 g^{-1})		Mesopore volume ($\cdot 10^{-3}$ cm^3 g^{-1})
		Adsorption	Desorption	
Calcium carbonate				
PCC	9.0	38	44	0.55
Chalk	2.1	8.8	12	
Titanium dioxide				
Anatase	7.83	26.0	32.8	0.57
Rutile	7.44	23.3	30.4	0.14
Rutile-Raw	8.90	25.6	31.1	0.61
Kaolin clay				
Kaolin-Cr	12.1	60.0	72.7	0.60
Kaolin-Am	21.6	129	152	1.2
Kaolin-Cr/Cal	11.4	46.2	52.8	0.50
Kaolin-Cal	13.7	52.1	61.0	0.28
Talc				
Talc-Prod	11.8	47.2	54.4	0.63
Talc-Raw	9.56	36.9	41.3	0.54

approach, the packed columns provided adequate flow and pressure drop for analyses to be performed [6].

2.2. Physical analysis

The specific surface area of each inorganic filler sample was determined by a multipoint BET method using nitrogen as the adsorbate in an ASAP 2000 (Micromeritics, Norcross, GA, USA). Samples were degassed at 200 °C for a minimum of 12 h before the surface area was measured. The results of these analyses are given in Table 1. A complete mesopore analysis was also performed using the ASAP 2000. The measured pore volumes, from adsorption and desorption data and estimations of mesopore volume are also provided in Table 1.

2.3. Inverse gas chromatography

A complete description of the methods used for IGC experiments is given elsewhere [6]. A HP5890 Series II gas chromatograph (Hewlett-Packard, now Agilent Technologies, Wilmington, DE, USA) with a flame ionization detector was used. The instrument was linked to a personal computer for instrument control and for data acquisition and data analysis. For each test, a known mass of about 10 g of aggregated inorganic filler was packed into a stainless steel column with a length of 60.0 cm and an internal diameter of 0.53 cm. High-purity (99.999%) nitrogen was used as the carrier gas to continually sweep the packed column at a rate of $\sim 23 \pm 0.2$ ml min^{-1} reagent-grade n-alkane probes, C_5–C_7, were injected in the low part per million range, i.e., Infinite Dilution. This was achieved by dilution with carrier gas using a method similar to that described by Ahsan et al. [25]. Methane gas, considered non-interacting with the surface, was used as an internal reference to determine the free volume of the column. The chromatographs for each probe were digitally recorded. The first moment of each peak was calculated and used as the probe retention time. Retention times were used to calculate the specific retention volumes, V_S^0, from which the surface energetic parameters were determined. Details of the theoretical development for calculating the apolar

component of the surface free energy, γ_S^{LW}, from V_S^0 may be found elsewhere [37].

2.4. Sample preconditioning

Two analysis techniques for IGC at infinite dilution were used in order to quantify the influence of water on the measured surface energies of the various filler samples. A discussion of the significance of results from the two methods, precondition analysis, and sequential isothermal analysis was reported earlier by Keller and Luner in their analysis of calcium carbonates [6]. In preconditioned analysis, which is the most widely applied method, the sample in the column was brought to equilibrium under a dry carrier gas purge at a preconditioning temperature, e.g., 100, 200 or 300 °C. The column temperature was then adjusted to the temperature at which IGC measurements were conducted, e.g., 100 °C. Probes were then injected and the retention times were recorded. In sequential isothermal analysis, measurement of probe retention times began once the freshly pack column was brought to measuring temperature, i.e., 100 °C, in the gas chromatograph oven. The changes in the test material that affect surface chemistry, such as the loss of water, were then monitored by the change in the elution time, i.e., the interaction of the probe with the surface.

3. Results and discussion

3.1. Titanium dioxide

The results of thermal preconditioned analysis of titanium dioxide samples are shown in Fig. 1, where the apolar component of surface free energy, γ_S^{LW}, is plotted as a function of conditioning temperature. The two crystal forms, Rutile and Anatase, exhibit a monotonic increase in γ_S^{LW}, from 60 to 70 mJ m^{-2} when preconditioned at 100 °C, to 105–165 mJ m^{-2} after conditioning at 300 °C. The γ_S^{LW} values observed for Anatase were consistently 10–20 mJ m^{-2} lower than those of Rutile conditioned at the same temperature. This small, but significant difference may arise from the chemistry of the exposed surface planes of the two crystalline forms. The Rutile
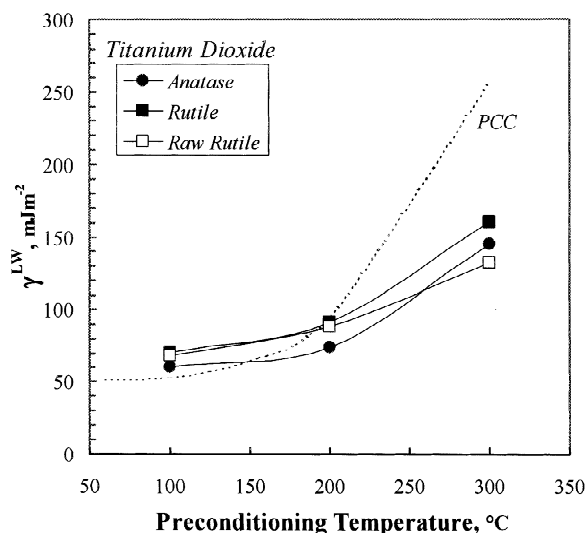
Fig. 1. Preconditioned IGC analysis of titanium dioxide samples. The apolar component of the surface free energy plotted as a function of preconditioning temperature, $T_c = 100\,^\circ C$.

product had a surface treatment of alumina. The Anatase had residual sulfate ions that remained after its synthesis reaction [35].

The results from testing the raw rutile sample are also illustrated in Fig. 1. At lower conditioning temperatures, γ_S^{LW} for Rutile (surface treated) and Rutile-Raw (untreated) were within experimental limits. At 300 °C, the γ_S^{LW} of Rutile is 30 mJ m^{-2} greater than the untreated Rutile-Raw sample. Treatment with alumina may create higher energy sites that are detected by the preconditioned IGC analysis.

The results from a previous study [6] of PCC are included for comparison in Fig. 1. The TiO$_2$ and CaCO$_3$ samples were found to have similar apolar surface energies after conditioning at 100 and 200 °C. After equilibrating at 300 °C the γ_S^{LW} for the TiO$_2$ samples were almost twice the values observed at 100 °C. The PCC had a much greater γ_S^{LW} (250 mJ m^{-2}) at 300 °C, which may result from changes in the surface associated with thermal decomposition and the formation of calcium oxide. Morimoto et al. [33] demonstrated that such decomposition of PCC becomes significant at temperatures exceeding 250 °C. Since TiO$_2$ is not subject to this type of decomposition, surface changes result only from the desorption of surface sorbed species, especially water. Surface water will be lost from desorption of

molecular water that is hydrogen bonded to oxygen or hydroxyl groups at the surface at temperatures from 25 to 150 °C. At temperatures up to ~350 °C, chemisorbed water, coordinated with the oxide groups will evolve [38].

Suda [34] calculated the change in electrostatic field strength of purified rutile associated with the desorption of surface water from heats of immersion experiments. In that work, the concentration of chemisorbed water, –OH groups nm^{-2}, was reduced from 7 (25 °C) to ~0.3 (300 °C). The respective electrostatic field strengths in statvolts cm^{-2} were ~0.2 (25 °C) and 1.5 (300 °C). This forms the basis for the model previously presented by Keller and Luner for calcium carbonates [6], where the induced dipole (Debye) component of the surface free energy has an increased contribution to the total energy due to the polarization of alkane molecules by the electric field at the surface. The presence of adsorbed water at lower conditioning temperatures dissipates the charge, thereby reducing the induced dipole interactions, and γ_S^{LW}.

The results for sequential isothermal analysis of hexane on the TiO$_2$ samples are shown in Fig. 2. In this figure, the specific retention volume, V_S^0, which is a direct function of the standard free energy of adsorption, ΔG_A^0, of n-hexane on the surface, is
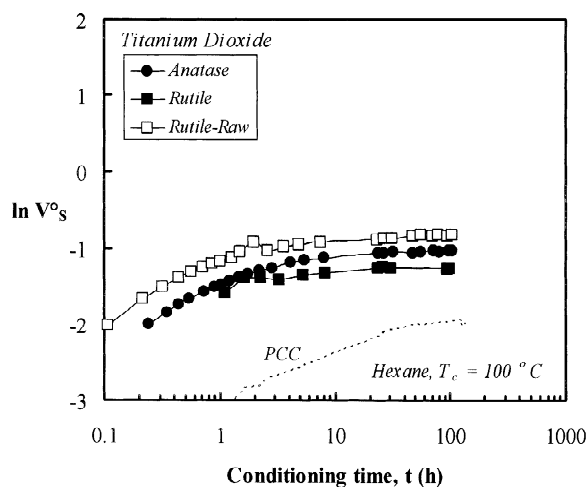

Fig. 2. Sequential isothermal IGC analysis of various titanium dioxide samples. Specific retention volume V_S^0, of hexane adsorbed on the surfaces of TiO$_2$ samples plotted as a function of conditioning time at 100 °C under a dry N$_2$ sweep.

plotted against conditioning time at 100 °C. All of the TiO_2 volume, V_S^0 of hexane adsorbed on the surfaces of TiO_2 samples plotted as a function of conditioning time samples undergo a significant increase in interaction energy up to about 10 h of conditioning. The magnitude of that increase was on the same order of that observed for the PCC sample, which is shown in Fig. 2 for comparison. After 10 h, very little change was observed for the TiO_2 samples suggesting they have effectively reached an equilibrium surface state. The differences between the three TiO_2 samples are not large enough to provide insight into differences in the surfaces, and may in fact result from experimental factors, e.g., column packing or aggregated particle morphology.

3.2. Kaolin clays

The kaolin clay samples studied in this investigation were selected to examine the effects of crystallinity and thermal structuring (calcination) on the apolar surface energetics. Fig. 3 shows the results for IGC preconditioning analysis of the kaolin samples. High values (>150 mJ m^{-2}) were observed for the well-crystallized, Kaolin-Cr, and amorphous (poorly crystallized), Kaolin-Am, samples over the range of temperatures tested. Both
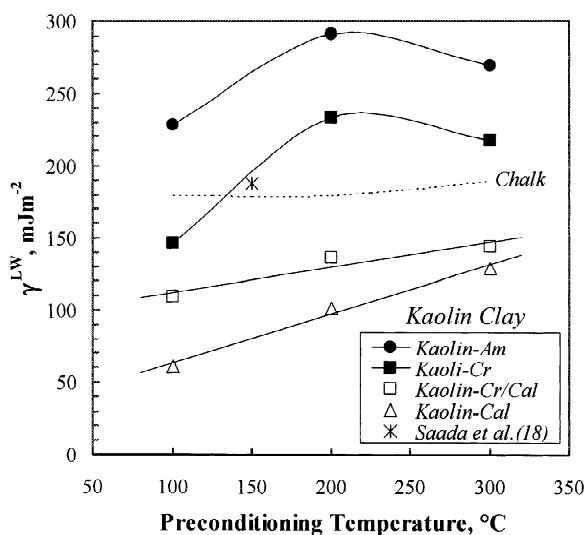

Fig. 3. Preconditioned IGC analysis of kaolin clay samples. The apolar component of the surface free energy plotted as a function of preconditioning temperature, $T_C = 100$ °C.

samples exhibited atypical behavior by having maximum γ_S^{LW} values at 200 °C. The γ_S^{LW} values were 5% lower when conditioned at 300 °C. The model proposed by Keller and Luner [6] may explain the increase in γ_S^{LW} from 100 to 200 °C where the loss of physisorbed molecular water exposes high-energy sites that increase the interaction energies of the probe molecules with the surface.

However, the unusual decrease in γ_S^{LW} between preconditioning of 200 and 300 °C is not adequately explained by that model. This behavior, unique to the non-calcined kaolin samples, may result from dehydration of the hydroxyl groups associated with the silica surface when heated above 200 °C. A similar trend was observed by Wade and Hackerman [39] using heats of immersion to examine kaolinite, although they observed an abrupt drop in surface energy at 380 °C. Crystalline water, bound within the sheet layers as hydroxyl groups should not be disturbed at the temperatures used in this study [40].

The amorphous sample gave consistently higher γ_S^{LW} values (50–75 mJ m^{-2}) compared to the well crystallized sample. The higher surface energy may result from ionic contaminants, e.g., iron compounds, on the surface. The Kaolin-Am sample has 0.98% Fe_2O_3 and 0.15% FeO, compared with 0.13% and 0.08%, respectively, for the Kaolin-Cr sample [41]. The Kaolin-Am sample is also known to have more surface and interlayer structural defects, which could increase apparent γ_S^{LW} in IGC. Fig. 3 includes the γ_S^{LW} results of Saada et al. [22] for a kaolinite with a surface area of 14 m^2 g^{-1}, which should be compared with Kaolin-Cr.

The values of γ_S^{LW} obtained for kaolin using IGC may be compared with values of γ_S^d determined for kaolinite using contact angle experiments by Janczuk and Bialopiotrowicz [42]. The methods they used to determine surface energies, i.e., dry and wet surface state, were also used in a previous study by Okayama et al. for calcium carbonate [43]. Table 2 gives the non-polar surface energy components for kaolin clays and calcium carbonates using the two approaches.

A comparison of the surface energies obtained from IGC and wetting for calcium carbonates was the subject of a report by Keller and Luner [7]. The surface energies obtained for kaolin/kaolinite, cf. Table 2, show a similar trend where γ_S^{LW} values

Table 2
Inorganic paper fillers

	Kaolin clay		Calcium carbonate	
	IGC	Wetting [42]	IGC [6]	Wetting [43]
Preconditioning temperature, °C	100	20	100	105
Surface energy, mJ m^{-2}				
γ_S^{LW}	150[†]		56	
	230[††]			
γ_S^{d} (water in alkane)		78		34
γ_S^{d} (alkane in water)		39		21

[†] Kaolin-Cr, well crystallized. [††] Kaolin-Am, amorphous.

from IGC are significantly higher than the γ_S^{d} values determined from the contact angle of a sessile drop of water formed on the surface in an alkane medium. The γ_S^{d} values determined from the contact angle of a sessile drop of alkane in a continuous medium of water are much lower still, likely due to the retention of a thin film of water on the surface that cannot be displaced by the alkane drop. They also gave an interpretation of the practical and theoretical differences between IGC and wetting results.

The results for the preconditioned analysis of thermally structured, or calcined, kaolin samples are also presented in Fig. 3. The γ_S^{LW} values for the laboratory calcination product of Kaolin-Cr increased with preconditioning temperature, from 110 mJ m^{-2} (100 °C) to 140 mJ m^{-2} (300 °C). These surface energies are much lower than for Kaolin-Cr sample. During the calcination process, the crystalline water, bound within the sheet structure will be expelled at temperatures greater than 500 °C, in addition to the adsorbed water which evolves at much lower temperatures. The layered structure also becomes more amorphous upon calcination [40]. It is postulated that the lower surface energies observed for the Kaolin-Cr/Cal are the consequence of either one or both occurrences. Considering the results for the Kaolin-Cr sample that underwent a decline in surface energy after preconditioning at temperatures greater than 200 °C, if that energy reduction was the result of irreversible dehydroxylation of the silica or alumina surface sites, then treatment at higher temperatures may be a continuation of that process to completion. Calcination at 900 °C will also involve the dehydroxylation of internal –OH groups bound within the structured layers. A second possible explanation of the lower surface energy values observed for the

Kaolin-Cr/Cal product may be that during the heating process, molecular water and hydroxyl groups are liberated, creating a highly energetic surface. On cooling in ambient conditions, the surface may be contaminated with adsorbates, other than water, that form stronger bonds with surface active sites. In preconditioning experiments, these sites remain covered and thus the surface remains at a lower surface energy.

The γ_S^{LW} values for the commercially calcined product, Kaolin-Cal, also shown in Fig. 3, are lower than those for the Kaolin-Cr/Cal, although both exhibit similar trends. The Kaolin-Cal contains dispersing additives that may account for the lower surface energies. The additives may occupy energetic sites on the surface, and are not desorbed at the preconditioning temperatures.

The results for sequential isothermal analysis using hexane to probe the kaolin clays are illustrated in Fig. 4. The magnitude of the specific retention volumes, V_S^{0}, for the different samples follows the same hierarchy as was observed for the apolar components of surface energy, cf. Fig. 3. The Kaolin-Am sample had the highest V_S^{0} values, an indication of high values for the standard free energy of adsorption of the alkane on the sample surface. The values of V_S^{0} for the Kaolin-Am sample were quite similar to those observed for the chalk sample [6]. The Kaolin-Cr sample displayed a similar increase in V_S^{0} with time as the Kaolin-Am, although values were substantially lower. The Kaolin-Cr/Cal showed similar behavior to the TiO$_2$ samples, cf. Fig. 2. The Kaolin-Cal samples showed a similar increase in values as the Kaolin-Cr and Kaolin-Am samples, although its V_S^{0} values are comparable to those observed for PCC [6].
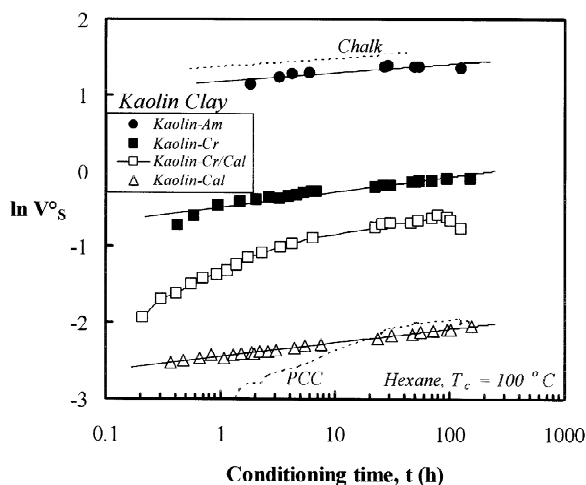
Fig. 4. Sequential isothermal IGC analysis of various kaolin clay samples. Specific retention volume V_s^0, of hexane adsorbed on the surfaces of kaolin samples plotted as a function of conditioning time at 100 °C under a dry N_2 sweep.

3.3. Talc

The results for the IGC preconditioned analysis of talc samples are presented in Fig. 5. The two samples that were tested were commercially prepared Talc-Prod that may have had milling aids or other
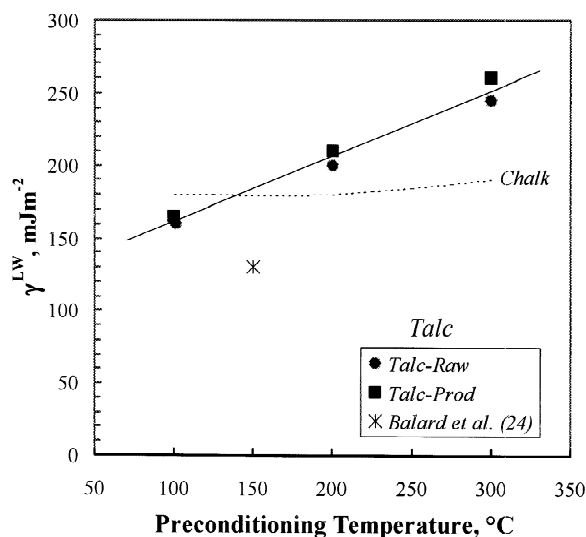

Fig. 5. Preconditioned IGC analysis of talc samples. The apolar component of the surface free energy plotted as a function of preconditioning temperature, $T_C = 100$ °C.

additives added during the manufacturing process, and Talc-Raw that was prepared by hand grinding the sample in the laboratory without additives. It is evident in the plot that the apolar components of surface free energy, γ_S^{LW}, for the two samples are similar. On preconditioning the values increase from 165 mJ m^{-2} (100 °C) to 250 mJ m^{-2} (300 °C). The results of chalk [6] are included in the figure for comparison. The surface energies are of the same magnitude as those observed for the kaolin clay samples (not calcined), cf. Fig. 3, although the talc samples do not exhibit an inflection point. The results obtained by Balard et al. [28] from IGC experiments are also plotted in Fig. 5. While the values for γ_S^{LW} observed in this study are 30 mJ m^{-2} higher than their results, both investigations found talc to exhibit a high-energy surface after thermal preconditioning.

The results for the sequential isothermal analysis of the talc samples show that the interaction of the alkane probes with the talc surfaces was relatively high and essentially constant over the course of 100 h with temperature held at 100 °C. This suggests that any dehydration that occurs at temperatures below 100 °C does so rapidly and at low temperatures.

4. Conclusions

In this investigation, the surface energetics of titanium dioxide, kaolin clays, and talc were studied using inverse gas chromatography. The apolar component of surface free energy, γ_S^{LW}, was determined by measuring the interaction of *n*-alkane probes with the mineral surfaces at infinite dilution. Preconditioned and sequential isothermal analyses were used to monitor the change in interaction and surface energy associated with dehydration on heating under a dry gas sweep.

Titanium dioxide samples were selected to test the significance of crystal structure and surface treatment. Rutile and Anatase samples gave similar response to preconditioning temperature exhibiting an increase of γ_S^{LW} from ~65 mJ m^{-2} (100 °C) to ~145 mJ m^{-2} (300 °C). This was a similar trend to what was previously observed with precipitated

calcium carbonate [7]. Although water loss at lower temperatures was presumed to account for the increase in γ_S^{LW}, it may be more appropriate to characterize the remaining hydroxyl population on the mineral surfaces. Rutile with no alumina surface treatment was also tested. It gave similar behavior to the rutile product at 100 °C, but exhibited lower γ_S^{LW} at temperatures up to 300 °C.

The kaolin clay samples that were tested in this study were chosen to study the affect of origin and crystallinity, and the impact of thermal structuring (calcination). Two standard clay samples, one well and one poorly crystallized were compared. Both exhibited high surface energies, although an unusual decrease in γ_S^{LW} was observed between 200 and 300 °C. The origin of this reversion was not established, although the behavior may result from dehydroxylation of sheet surface sites, or a collapse of the structure. The conditioning temperatures were too low for crystalline water to evolve. Calcined samples were tested and found to have substantially lower surface energies over the entire temperature range, as compared to untreated kaolin samples. It was postulated that this resulted from the irreversible dehydroxylation of the structure, or the tenacious adsorption of contaminates onto the high-energy sites.

Talc that was obtained from a commercial product and from a mineralogical specimen were compared. Little difference was observed between the samples in the IGC analyses. Both demonstrated relatively high apolar surface energies that increased with preconditioning temperature from 160 mJ m^{-2} (100 °) to 250 mJ m^{-2} (300 °C). Sequential isothermal results indicate that any change in surface energy up to 100 °C must occur at lower temperatures and very rapidly.

It was demonstrated that inverse gas chromatography is a useful tool for characterizing the surface energetics of various papermaking filler/pigments in their powdered state. The importance of water loss to the measured surface energy was also presented. Characterization of the interaction of the surfaces with water, and control of the water layers to replicate conditions in the final composite structure represent an important potential for understanding adhesion and wetting behavior. The characterization of molecular water and bound hydroxyl groups on the surfaces of composite materials may also be essential to this understanding.

5. Nomenclature

a	Cross sectional area of the methylene group, 6 Å^2
A_{sp}	Specific surface area, m^2 g^{-1}
F_{col}	Flow-rate of carrier gas, cm^3 s^{-1}
j	James–Martin correction for compressibility
ΔG_A^0	Standard molar free energy of adsorption, kJ mol^{-1}
$\Delta G_A^{CH_2}$	Incremental change in free energy per methylene group, kJ mol^{-1}
K_S	Henry's Law constant
N	Avogadro's constant, mol^{-1}
R	Gas constant
t_p	Retention time of test probe, s
t_m	Retention time of marker probe, s
T_C	Column temperature, K
V_g^0	Specific retention volume, per unit of adsorbent mass, cm^3
V_S^0	Specific retention volume, per unit of adsorbent surface area, cm^3
w	Mass of absorbent, g
γ_S^{LW}	Lifshitz–Van der Waals contribution to the surface free energy, mJ m^{-2}
γ_S^d	London (dispersive) contribution to the surface free energy, mJ m^{-2}
γ_S^i	Debye (dipole–induced dipole) contribution γ_S^{LW}, mJ m^{-2}
γ_S^μ	Keesom (dipole–dipole) contribution to γ_S^{LW}, mJ m^{-2}
γ_{CH_2}	Surface energy of polyethylene, mJ m^{-2}

Acknowledgements

References

[1] H.L. Lee, P. Luner, Nordic Pulp Paper Res. 4 (1989) 164.

[2] H.L. Lee, P. Luner, J. Colloid Interface Sci. 146 (1991) 195.
[3] D.P. Kamdem, S.K. Bose, P. Luner, Langmuir 9 (1993) 3039.
[4] D.P. Kamdem, B. Riedl, J. Wood Chem. Technol. 11 (1991) 57.
[5] M. Pyda, M. Sidqi, D.S. Keller, P. Luner, Tappi J. 76 (1993) 79.
[6] D.S. Keller, P. Luner, Colloids Surfaces A 161 (2000) 401.
[7] D.S. Keller, P. Luner, in: C.F. Baker (Ed.), The Fundamentals of Papermaking Materials: Transactions of the 11th Fundamental Research Symposium Cambridge, September 1997. PIRA International, Leatherhead, UK, 1997, p. 911.
[8] A. Lundqvist, L. Odberg, J.C. Berg, Tappi J. 78 (1995) 139.
[9] H. Al-Turail, W. Unertl, P. Lepoutre, J. Adhesion Sci. Technol. 9 (1995) 801.
[10] A. Lundqvist, L. Odberg, J. Pulp Paper Sci. 23 (1997) 298.
[11] P. Lepoutre, M. Inoue, J. Asple, Tappi J. 68 (1985) 86.
[12] G. Garnier, W.G. Glasser, J. Adhesion 46 (1994) 165.
[13] G.M. Dorris, D.G. Gray, J. Colloid Interface Sci. 77 (1980) 353.
[14] N. Gurnagul, D.G. Gray, Can. J. Chem. 65 (1987) 1935.
[15] S.L. McArthur, Thermodynamic Properties of Solvents at Infinite Dilution in Lignin, Michigan State University, 1987.
[16] D.S. Keller, P. Luner, in: L. Schroeder (Ed.), Report to the Empire State Paper Research Associates, Report 99, SUNY-ESF, Syracuse, NY, 1992, p. 25.
[17] R.J. Good, M.K. Chaudhury, in: L.-H. Lee (Ed.), Fundamentals of Adhesion, Plenum Press, New York, 1991.
[18] F.M. Fowkes, J. Colloid Interface Sci. 28 (1968) 493.
[19] J.C. Berg, in: J.C. Berg (Ed.), Wetting, Marcel Dekker, New York, 1993, p. 140.
[20] T. Morimoto, Y. Suda, Langmuir 1 (1985) 239.
[21] H. Balard, A. Saada, E. Papirer, B. Siffert, Langmuir 13 (1997) 1256.
[22] A. Saada, E. Papirer, H. Balard, B. Sifert, J. Colloid Interface Sci. 175 (1995) 212.
[23] H. Hadjar, H. Balard, E. Papirer, Colloids Surfaces A 99 (1995) 45.
[24] E. Papirer, J. Schultz, C. Turchi, Eur. Polym. J. 20 (1984) 1155.
[25] T. Ahsan, B.A. Colenutt, K.S.W. Sing, J. Chromatogr. 464 (1989) 416.
[26] M.A. Rodriquez, J. Rubio, M.J. Liso, J.L. Oteo, Clays Clay Minerals 45 (1997) 670.
[27] H. Balard, O. Aouadj, E. Papirer, Langmuir 13 (1997) 1251.
[28] H. Balard, P. Uhlmann, O. Aouadj, F. Clauss, R. Baeza, E. Papirer, in: Proceedings of Eurofillers 95, International Conference, Mulhouse, 1995, p. 9.
[29] G.M. Dorris, D.G. Gray, J. Phys. Chem. 85 (1981) 3628.
[30] H. Balard, A. Saada, B. Siffert, E. Papirer, Clays Clay Minerals 45 (1997) 489.
[31] T. Morimoto, M. Nagao, J. Imai, Bull. Chem. Soc. Japan 44 (1971) 1282.
[32] T. Morimoto, M. Nagao, F. Tokuda, J. Phys. Chem. 73 (1969) 243.
[33] T. Morimoto, J. Hishi, O. Okada, T. Kadota, J. Phys. Chem. 53 (1980) 1918.
[34] Y. Suda, Langmuir 3 (1987) 1119.
[35] R. Hagemeyer, Pigments for Paper, Tappi Press, Atlanta, GA, 1997.
[36] R.J. Pruett, H.L. Webb, Clays Clay Minerals 41 (1993) 514.
[37] D. Atkinson, G. Curthoys, J. Chem. Educ. 55 (1978) 564.
[38] G.D. Parfitt, in: J.F. Danielli et al. (Eds.), Progress in Surface and Membrane Science, Vol. 11, Academic Press, 1976, p. 181.
[39] W.H. Wade, N. Hackerman, J. Phys. Chem. 63 (1959) 1639.
[40] B. Velde, Introduction to Clay Materials: Chemistry, Origins, Uses and Environmental Significance, Chapman and Hall, New York, 1992.
[41] H. VanOlphen, J.J. Fripiat, Data Handbook for Clay Materials and Other Non-Metallic Minerals, Pergamon Press, New York, 1979.
[42] B. Janczuk, T. Bialopiotrowicz, Clays Clay Minerals 36 (1988) 243.
[43] T. Okayama, D.S. Keller, P. Luner, J. Adhesion 63 (1997) 231.